Available online at www.sciencedirect.com
SCIENCE DIRECT®
ELSEVIER
Nuclear Instruments and Methods in Physics Research A 554 (2005) 291–299
NUCLEAR INSTRUMENTS & METHODS IN PHYSICS RESEARCH Section A
www.elsevier.com/locate/nima

Characteristics of depth-sensing coplanar grid CdZnTe detectors

Zhong He*, Ben W. Sturm

Department of Nuclear Engineering and Radiological Sciences, University of Michigan, Ann Arbor, MI 48109, USA

Received 10 October 2004; received in revised form 30 May 2005; accepted 9 June 2005
Available online 20 July 2005

Abstract

The latest depth-sensing coplanar grid CdZnTe detectors have been tested. Two of these have dimensions $1.5 \times 1.5 \times 1.0\,cm^3$ and one is a cylindrical detector with 1.5 cm diameter and 1.0 cm length, all of them using the third-generation coplanar anode design. Energy resolutions of 2.0% and 2.4% FWHM at 662 keV γ-ray energies were obtained. Detector performance has been observed experimentally as a function of depth of the γ-ray interaction, and as a function of radial position near the anode surface. The measured results show the improvement of the third-generation anode design. Material uniformity of CdZnTe crystals manufactured by eV Products have been directly observed and compared on two $1.5 \times 1.5 \times 1.0\,cm^3$ detectors.

Keywords: Coplanar grid; CdZnTe; Depth-sensing; γ-ray spectroscopy; Semiconductor detector

1. Introduction

Room temperature semiconductor devices used for γ-ray detection have long been studied because of their superior charge carrier statistics in comparison to gas and scintillation detectors. Such semiconductors include CdZnTe, CdTe, and HgI_2, all having a wide band gap and a high atomic number. However, these materials had been limited in use to thin detectors due to their poor hole mobilities. In 1994, Luke [1] developed a single polarity charge sensing technique that worked in a manner analogous to the Frisch grid [2] configuration in gas ion chambers. Luke's technique employed parallel strips that were connected in an alternate manner, producing two sets of inter-digital grid electrodes, or coplanar grid electrodes. The read-out of this system was done in a fashion, by subtracting the coplanar signals, to produce a net signal dependent only on the movement of charge carriers near the coplanar electrodes. In this way, the coplanar grid detector can act as a single polarity charge-sensing device. When the coplanar electrodes are biased to collect

*Corresponding author. Tel.: +1 734 764 7130; fax: +1 734 763 4540.
E-mail address: hezhong@umich.edu (Z. He).

0168-9002/$ - see front matter © 2005 Elsevier B.V. All rights reserved.
doi:10.1016/j.nima.2005.06.064

electrons, the effects of poor hole mobility can be mitigated.

To compensate for electron trapping, Luke [1] employed a linear compensation technique using a subtraction circuit with a relative gain applied between the two channels. This method compensates for electron trapping assuming good material uniformity throughout the whole crystal. In 1996, He et al. [3,4] proposed a method using depth-sensing to correct for electron trapping. This method uses signals from the cathode and coplanar anodes to determine the depth of the γ-ray interaction. In this way, spectra can be obtained as a function of interaction depth, allowing one to compensate for electron trapping for any depth-dependent function.

In the early coplanar grid designs, He et al. [3] observed significant energy resolution degradation near the coplanar anodes, which was later attributed to the weighting potential non-symmetric effect [5,6]. Based on this understanding, He et al. [5] proposed using a boundary electrode surrounding the coplanar anodes which would aid in balancing the weighting potentials along the edges of the detector. With this new design, named generation 2, the difference of the weighting potentials along the edge of the detector was significantly reduced. Still, the anode geometry was not optimized, and so a generation 3 design was proposed [5]. In this design, the strip widths of the two outermost grids and three outermost gaps were fine-tuned in order to minimize the difference of the weighting potential about the area of the detector.

In this paper, we discuss the performance improvements with the generation 3 coplanar electrode design.

2. Third-generation coplanar anode design

It has been observed that the design of the coplanar anode geometry has a significant effect on detector performance. When the weighting potentials of the coplanar anodes are insufficiently balanced, events occurring near the coplanar anodes will result in a degraded energy resolution. To circumvent the problem of non-symmetric weighting potentials, He et al. [5] proposed a generation 3 design as shown in Fig. 1. This anode geometry involves a coplanar anode grid structure surrounded by a boundary electrode. The purpose of the boundary electrode is to aid in balancing the weighting potentials for both coplanar anodes. This is because, when the weighting potential of the collecting anode is calculated, a unit potential is assigned to the collecting anode and 0 potentials are assigned to all other electrodes. When the boundary electrode is excluded, the boundary conditions force an imbalance in the potential near the periphery of the anode surface, because the most outside strip electrode will have either a 1 or 0 weighting potential, but not both. With the addition of the boundary electrode, the potential is fixed to 0 along the periphery of the anode surface, making it possible to balance the weighting potentials of the two central coplanar anodes.

The generation 3 design was improved from the generation 2 design by changing the widths of the two outermost strips and three outermost gaps. The basis behind this change was the effect of the potential field around the perimeter of the detector being dominated by the outermost anode strip. By reducing the width of the outermost strip and increasing the width of the second outermost strip, a much more balanced weighting potential profile can result. The generation 3 design was modeled using the electrostatic finite-element analysis software package Maxwell [7] and the design improvements were verified by simulations.

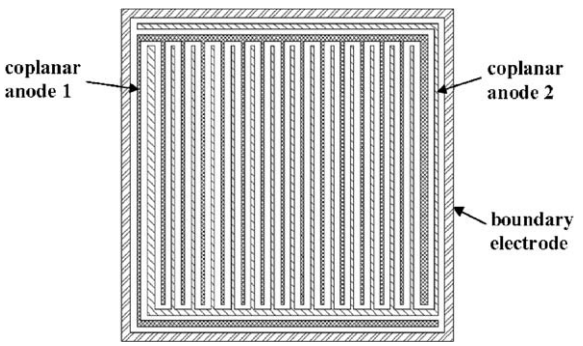

Fig. 1. Generation 3 coplanar grid design consisting of two coplanar anodes and a boundary electrode.

3. Principles of depth and radial-sensing

3.1. Depth-sensing technique using cathode/anode ratio

A novel method to determine the depth of a γ-ray interaction was proposed in [3]. This method utilizes the linear shape of the cathode weighting potential, resulting in a depth-dependent cathode signal (C) that can be expressed as $C \propto D\,E_\gamma$, where D is the distance from the coplanar anodes and E_γ is the energy deposited by the incident γ-ray. The coplanar anode signal, on the other hand, is proportional to the energy deposited (assuming the relative gain is set to 1 and the weighting potential difference is 0 from the cathode side up to one pitch length from the anode side). Hence, the coplanar anode signal (A) can be expressed as $A \propto E_\gamma$. It is then evident that by taking the ratio of the cathode and coplanar anode signals, i.e., $d = C/A \propto D$, the interaction depth D can be determined. Depth-sensing allows us the capability of producing spectra as a function of interaction depth.

3.2. Radial sensing near the anode surface

The technique of radial sensing in coplanar grid detectors was explained in [5]. In this technique, we employ the convex nature of the collecting anode weighting potential, in the lateral direction for a fixed depth, to determine the relative radial position of a γ-ray interaction. The induced charge on an electrode due to the movement of a single charge carrier is proportional to the difference of the weighting potential between the beginning and end positions of the charge's path. Since the weighting potential of the collecting anode is greater in the center (W_{center}) than it is along the periphery (W_{edge}) at a specific depth Z, and the weighting potential on the anode surface where the electrons are collected is 1, then the induced charge on the collecting anode (Ac) will be larger for events starting near the periphery than for events starting near the center. This effect is illustrated in Fig. 2. Using this information, we can obtain the relative radial position of an event

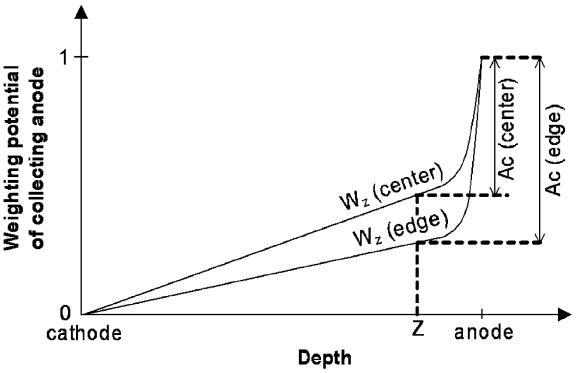

Fig. 2. Induced charge of a single electron formed at depth Z, at two different radial positions, and traveling to the collecting anode.

using the following relationship:

$$\frac{\text{Ac(edge)}}{(\text{Ac}-\text{Anc})} > \frac{\text{Ac(central)}}{(\text{Ac}-\text{Anc})}$$

where the coplanar anode signal (Ac–Anc) is taken with the relative gain set to 1. This technique allows us to obtain spectra as a function of radial position.

4. Detector performance

4.1. Methods of operation

Coplanar grid detectors with boundary electrodes can be operated in two modes. When the non-collecting anode and the boundary electrode are biased at the same potential, lower than that of the collecting anode, electrons generated in the whole detector volume will be collected by the collecting anode. Alternatively, the collecting anode can be biased to the same potential as the boundary electrode, while the non-collecting anode is set to a lower potential. This results in the collection of electrons by the boundary electrode when charges are generated near the sides of the detector. Only electrons generated in the central region of the device can be collected by the collecting anode, where the difference of weighting potentials of coplanar anodes is minimum. Therefore, the detector performance is expected to be better in the later mode of operation since the charge

induced from electrons formed in the central region of the detector will be more uniform.

Depth-sensing results obtained using a $1.5 \times 1.5 \times 1.0\,cm^3$ generation 3 detector under these two modes of operation are illustrated in Fig. 3. Our experimental results show a typical degradation of about 0.2% FWHM when the full detection volume is active to radiation while the detection efficiency is about 25% higher [8]. This shows the detector performance is worse near the periphery of the devices.

4.2. Depth-sensing results

A total of three detectors were ordered from eV Products [9]. Two of these were parallel epipeds with dimensions $1.5 \times 1.5 \times 1.0\,cm^3$ and consisted of a square electrode design similar to that in Fig. 1. These were designated as MO2 2-2 square and MO2 2-3 square. The other detector was cylindrical in shape 1.5 cm in diameter and 1.0 cm in length. This detector was designated as MO2 2-2 cylindrical and consisted of a circular electrode design with electrodes in the shape of a concentric helix. The cylindrical design was tested to determine if the circular shape of the electrodes could help to mitigate edge effects that would be present on the square design.

Using the depth-sensing method, energy resolutions between 2.0% and 2.1% FWHM at 662 keV for the MO2 2-2 square detector were consistently achieved. The performance for the other two detectors was not as notable. Using the MO2 2-3 square detector an energy resolution of ~2.4% was achieved, whereas the MO2 2-2 cylindrical detector resulted in an energy resolution of ~2.5%.

4.3. Validation of improved electrode design

To verify the improvement of the anode design, pulse height spectra as a function of depth were obtained on two detectors, one using eV Product's generation 2 design, where all strips and gaps had constant widths [8], and the other using UM's generation 3 design. Fig. 4(a) shows the spectrum obtained at each depth for the generation 2 design. We observe that the photopeak resolution is best near the cathode side of the detector and worse near the coplanar anode surface. This phenomenon is the result of the weighting potential non-symmetry rather than charge trapping, because the effect of charge trapping should be most severe towards the cathode side. Fig. 4(b) shows the same measurement using the detector with the generation 3 design. In contrast, the spectra show better resolution near the coplanar anodes. A direct comparison of energy resolution as a function of interaction depth for the two different electrode designs is illustrated in Fig. 4(c). The fact that the generation 3 design showed no degradation near the coplanar anodes supports our theory that the new design is superior.

5. Measurement results for radial sensing

Results using radial sensing for three detectors with different anode designs are shown in Fig. 5. The spectra shown in these figures are taken at different radial positions at about the same interaction depth, near the coplanar anodes. These spectra indicate the charge induction uniformity for electrons formed at different radial positions within the detector.

5.1. Second-generation design

The spectra obtained in Fig. 5(a) confirm the severity of the non-symmetric weighting potential in the generation 2 design. These results show that the deviation of the photopeak centroid position from that of the center region of the detector increases with increasing radial position. The amount of deviation in the photopeak position is ~5–6%.

It is also clear from Fig. 5(a) that multiple peaks were observed for spectra 2 and 3. This can be explained based on the design of Fig. 1, which can be used as an example in our discussion on the generation 2 detector. In Fig. 1, if the events are generated on the left-hand side of the device near the anode surface, the weighting potential of the collecting anode (coplanar anode 1) is higher than that of the non-collecting anode (coplanar anode 2) due to the closer proximity of the collecting

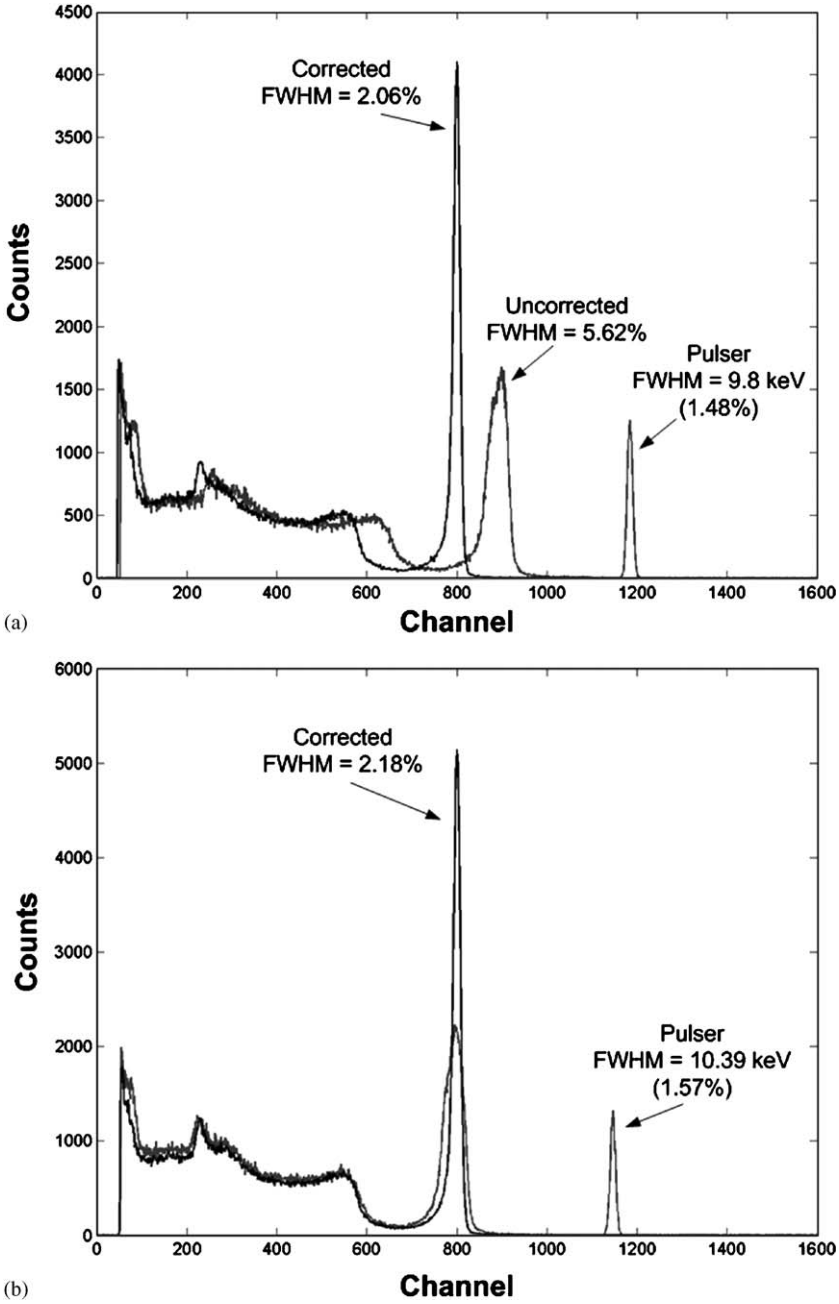

Fig. 3. Cs-137 spectrum obtained using an eV Products MO2 2-2 square detector utilizing the depth-sensing method where (a) is taken with the cathode set to −1700 V, the non-collecting anode set to −80 V, and the collecting anode and boundary electrode are set both at ground and (b) is taken with the cathode set to −1600 V, the collecting anode set to +80 V, and in this case the non-collecting anode and boundary electrode are both set to ground. Condition (a) results in only the electrons generated in the central region being collected by the coplanar anodes, whereas, in (b) electrons generated in the whole device are collected by the coplanar anodes.

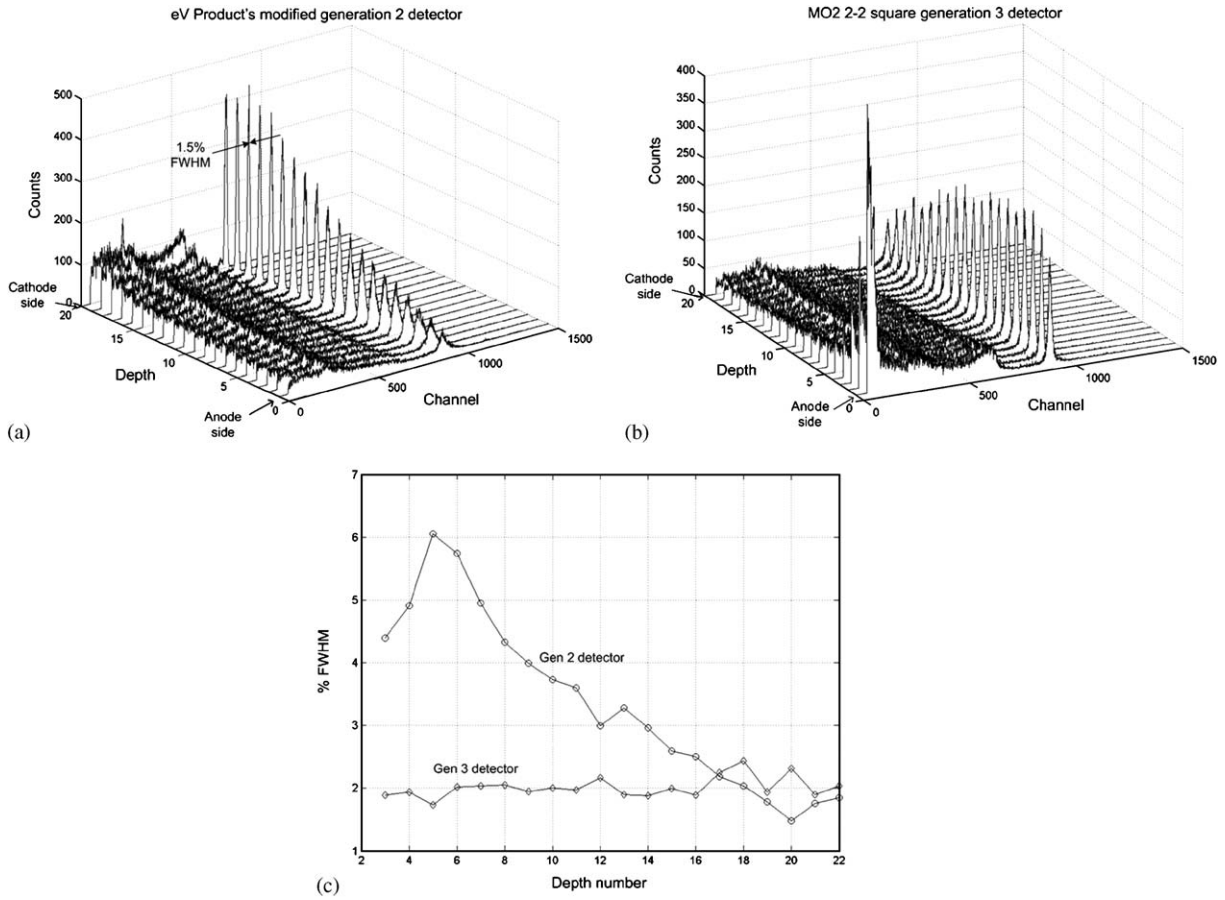

Fig. 4. Energy spectra at each depth using a Cs-137 γ-ray source for (a) the eV Product's generation 2 detector and (b) the generation 3 detector, both spectra were taken with a cathode bias of -1700 V and anode bias of -80 V. The plot in (c) shows the energy resolution (% FWHM) as a function of the interaction depth for both electrode configurations.

anode to the boundary electrode. Therefore, the weighting potential of the coplanar signal (W_c–W_{nc}) is higher than that in the central region. This causes the induced coplanar signal to be smaller than for those events produced in the central region. Similarly, if the events are formed on the right-hand side of the device, the coplanar signal is larger. These variations in the weighting potentials cause the double-peak feature as shown in Fig. 5(a), spectrum 2. It can be imagined that when the interaction position shifts from the left side of the detector to the right side, the amplitude of the coplanar signal will change from lower to higher values. In some intermediate regions, such as the top or bottom of the device, the weighting fields of the collecting and non-collecting anodes may be very close. This results in a third peak in the middle, as shown in Fig. 5(a), spectrum 3.

Another important feature in Fig. 5(a) is the shift towards lower energy in the peak centroid position for spectrum 4. This spectrum constitutes events that occur at the largest radial position. The reason why events occurring in this region are shifted to a lower channel number can be explained based on Fig. 6. This plot shows the weighting potential for the collecting anode and non-collecting anode on a generation 2 detector at a depth of 1 mm from the anode surface. Suppose the radial index value at

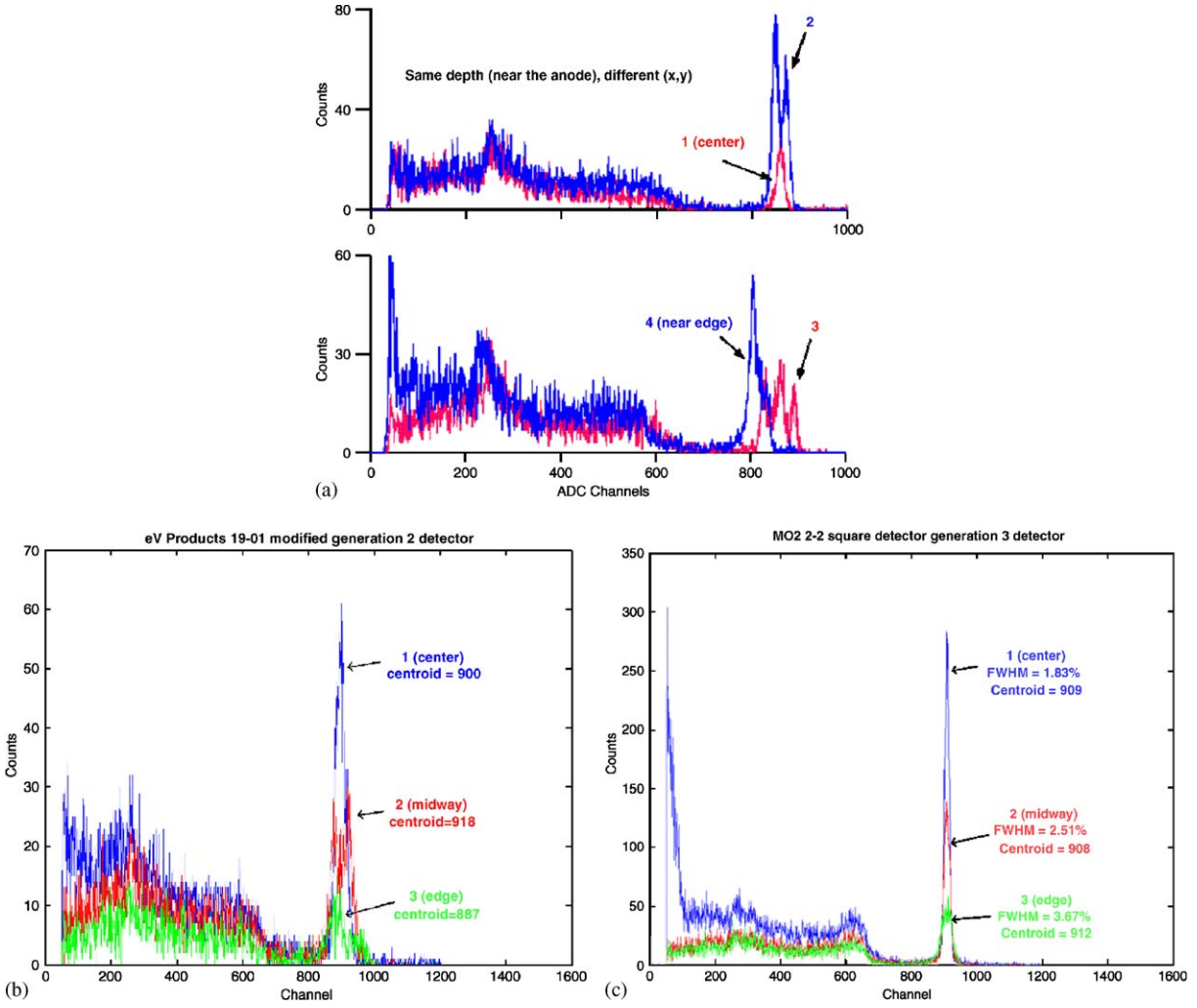

Fig. 5. Cs-137 spectra taken at different radial positions at one particular interaction depth for (a) the generation 2 detector, where spectra numbers 1–4 indicate increasing radial positions (b) the I9-01 detector with eV's generation 2 design and (c) the MO2 2-2 square detector with the generation 3 design, where both (b) and (c) were taken with a cathode bias of −1700 V and anode bias of −80 V. In (b) and (c), numbers 1→2→3 indicate increasing radial positions.

position 1 (R_1) is given by

$$R_1 = \frac{\mathrm{Ac}}{\mathrm{Ac} - \mathrm{Anc}}. \quad (1)$$

If the difference of the collecting anode and non-collecting anode at position 1 is $+D$, then the difference at position 2 is $-D$, assuming positions 1 and 2 are equidistant to the center of the device. The weighting potential of the collecting anode at position 2 is shifted lower by D and hence the collecting anode signal will be greater by D. Likewise, the weighting potential of the coplanar signal at position 2 is shifted lower by $2D$ and hence the coplanar signal will be greater by $2D$. Therefore, the radial index value at position 2 (R_2) is given by

$$R_2 = \frac{\mathrm{Ac} + D}{\mathrm{Ac} - \mathrm{Anc} + 2D}. \quad (2)$$

It can be found that $R_1 > R_2$ if $\mathrm{Ac} > -\mathrm{Anc}$. That is, if the collecting anode signal is greater than the negative component of the non-collecting anode

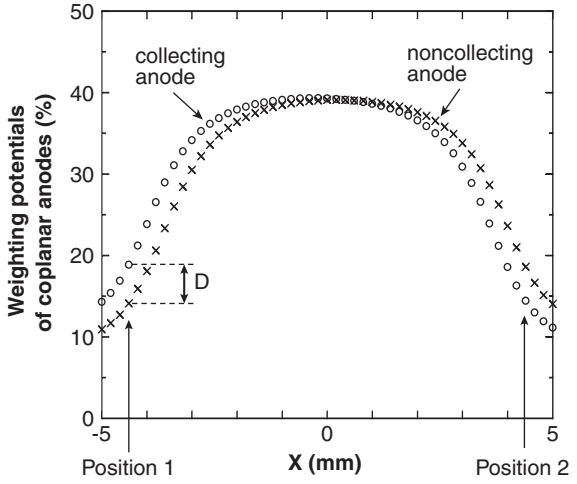

Fig. 6. Plot depicting the effect of reduced pulse height for events occurring at the largest radial position. The data points shown indicate the weighting potential of the coplanar anodes on a generation 2 detector along a center section of the device at a depth of 1 mm from the anode surface.

signal, then position 1 will have a larger radial index value than position 2. This inequality will hold for all events occurring at depths greater than 1 pitch (~1 mm) from the anodes. Events occurring at position 1 will have smaller pulse amplitude, because the coplanar weighting potential at this position is some finite positive value. Hence, the largest radial position events will give rise to a smaller peak centroid value.

5.2. eV Product's design

For the modified generation 2 design, as described in [8], the effects of a non-symmetric weighting potential are evident in Fig. 5(b), which are not as severe as in the previous case, but are still substantial. A shift of ~2% in the photopeak centroid position was observed. Also, multiple peaks for radial position 2 were again observed in addition to a low-energy peak shift for radial position 3. All of these effects provide additional evidence of the weighting potential non-symmetric effect, resulting in the poor spectroscopic performance near the coplanar anodes.

When the weighting potentials of the coplanar anodes are not symmetric, the difference is a maximum near the periphery and a minimum in the central region. Therefore, by observing the difference of detector performance in the central region and near the periphery (larger radial coordinates), we can observe the improvement of our overall design symmetry between the weighting potentials, since the variation of charge generation and material properties are not likely to depend solely on the radial coordinates.

5.3. Third-generation design

The radial spectra for the generation 3 design are shown in Fig. 5(c). We observe a much sharper photopeak than in the previous two detectors and a much smaller deviation of the photopeak position. The magnitude of this deviation is ~0.3%. Also, multiple peaks were not observed for this device. This confirms that the difference in the weighting potentials has been significantly reduced.

6. Material uniformity

The depth-sensing method gives us the capability to obtain information about the detector that is not available using the conventional coplanar grid readout technique. In Fig. 4(a), we observed a poorer energy resolution of 6.1% FWHM near the anode side of the detector and a very good resolution of 1.5% FWHM near the cathode side. This indicates that the electron trapping does not degrade energy resolution significantly, because electrons with larger drift distances are more susceptible to the non-uniformity of charge trapping sites. However, the best energy resolution was observed for events occurring on the cathode side, suggesting the material's good charge transport properties for electrons. In contrast, the energy resolution on the MO2 2-2 square detector in Fig. 4(b) was slightly poorer near the cathode side than it was near the anode side, suggesting that the transport of electrons through the detector material degrades the resolution towards the cathode side. This observation was consistent with what was reported by eV Products. That is, the dimensions of Te inclusions were larger in the

crystals used for the newest generation 3 detectors. The link between degraded energy resolution and the concentration of Te inclusions has been reported previously [10,11].

7. Summary

The experimental results show the improvement in detector performance obtained using the generation 3 coplanar grid design. Using the depth-sensing method, consistently good energy resolutions of 2.0–2.1% FWHM at 662 keV were achieved on one detector. Using the radial sensing method, we showed the deleterious effects of a non-symmetric weighting potential and the improvement that resulted with the generation 3 design. We observed with depth-sensing the difference in material characteristics of two crystals. One crystal has better electron transport properties than the other. This shows that the quality of CdZnTe materials and the design of coplanar anodes both affect the performance of coplanar grid detectors.

Acknowledgment

We thank José Manuel Pérez of CIEMAT, Spain for his design work on the third-generation coplanar grid anodes used on the latest CdZnTe detectors. This project was supported by US Department of Energy NA-22 office under award number: DE-FG52-01-NN20122.

References

[1] P.N. Luke, IEEE Transactions on Nuclear Science 42 (1995) 207.
[2] O. Frisch, British Atomic Energy Report, vol. BR-49, 1944.
[3] Z. He, G.F. Knoll, D.K. Wehe, R. Rojeski, C.H. Mastrangelo, M. Hammig, C. Barrett, A. Uritani, Nuclear Instruments and Methods in Physics Research Section A: Accelerators, Spectrometers, Detectors and Associated Equipment 380 (1996) 228.
[4] Z. He, G.F. Knoll, D.K. Wehe, J. Miyamoto, Nuclear Instruments and Methods in Physics Research Section A: Accelerators, Spectrometers, Detectors and Associated Equipment 388 (1997) 180.
[5] Z. He, G.F. Knoll, D.K. Wehe, Y.F. Du, Nuclear Instruments and Methods in Physics Research Section A: Accelerators, Spectrometers, Detectors and Associated Equipment 411 (1998) 107.
[6] P.N. Luke, M. Amman, T.H. Prettyman, P.A. Russo, D.A. Close, IEEE Transactions on Nuclear Science 44 (1997) 713.
[7] "Maxwell 3D", Ansoft, Four Station Square, Suite 200, Pittsburgh, PA 15219, USA.
[8] J.M. Perez, Z. He, D.K. Wehe, Y.F. Du, IEEE Transactions on Nuclear Science 49 (2002) 2010.
[9] eV Products, 375 Saxonburg Boulevard, Saxonburg, PA 16056, USA.
[10] M. Amman, J.S. Lee, P.N. Luke, Journal of Applied Physics 92 (2002) 3198.
[11] C. Szeles, IEEE Transactions on Nuclear Science 51 (2004) 1242.